

## DEFECTIVE STRUCTURE OF SILICON DOPED WITH DYSPROSIUM

 Khodjakbar S. Daliev<sup>a</sup>,  Sharifa B. Utamuradova<sup>b</sup>,  Alisher Khaitbaev<sup>b</sup>,  
 Jonibek J. Khamdamov<sup>b</sup>,  Shahriyor B. Norkulov<sup>b\*</sup>,  Mansur B. Bekmuratov<sup>c</sup>

<sup>a</sup>Branch of the Federal State Budgetary Educational Institution of Higher Education “National Research University MPEI”,  
1 Yogdu st., Tashkent, Uzbekistan

<sup>b</sup>Institute of Semiconductor Physics and Microelectronics at the National University of Uzbekistan,  
20 Yangi Almazar st., Tashkent, 100057, Uzbekistan

<sup>c</sup>Nukus State Pedagogical Institute named after Ajiniyaz, Nukus, Uzbekistan

\*Corresponding Author e-mail: [nshb19990@gmail.com](mailto:nshb19990@gmail.com)

Received March 02, 2024; revised April 6, 2024; accepted April 8, 2024

In this work, the structural and optical characteristics of silicon (n-Si) samples and its compositions with dysprosium (n-Si-Dy) were analyzed using Fourier transform infrared spectroscopy (FTIR) and Raman spectroscopy methods. Characteristic peaks in the FTIR spectra such as  $640\text{ cm}^{-1}$  (Si-H mode) and  $1615\text{ cm}^{-1}$  (perpendicular stretching mode) were identified, indicating the structural features of the material. The appearance of additional peaks in the n-Si-Dy spectra at  $516.71\text{ cm}^{-1}$  and  $805\text{ cm}^{-1}$  indicates the influence of dysprosium on the structure and defectiveness of the material. Examination of the frequency range ( $1950\text{--}2250\text{ cm}^{-1}$ ) further confirms local vibration modes associated with defects and interactions with dysprosium. Peaks associated with Dy-Dy stretching, as well as interaction with silicon, were found at  $2110\text{ cm}^{-1}$  and  $2124\text{ cm}^{-1}$ . Analysis of Raman spectra indicates the formation of silicon nanocrystals during annealing, which is confirmed by XRD results. The results obtained provide important insight into the effect of dysprosium on the structure and properties of silicon materials, which could potentially find application in optoelectronics and materials science.

**Key words:** Silicon, Dysprosium, Rare earth elements, Raman scattering, Diffusion, Heat treatment, Temperature

**PACS:** 33.20.Ea, 33.20.Fb

### INTRODUCTION

Although crystalline silicon plays a critical role in the microelectronics industry, its use in optoelectronics faces limitations due to its indirect bandgap semiconductor properties, which reduces the efficiency of emitting light in the visible spectrum. The discovery of strong visible photoluminescence in porous silicon at room temperature [1] has stimulated active research into the development of structures, including silicon nanowires and nanoparticles, as well as the study of their structural and optoelectronic characteristics.

Further studies showed pronounced visible light emission from nanocrystalline silicon films [2] and thin  $\text{SiO}_2$  films containing both crystalline [4] and amorphous [5] silicon nanoparticles. This luminescence is often attributed to the radiative recombination of charge carriers within Si nanoparticles, and its color can be controlled by varying the size of the nanoparticles [21]. Later, intense visible photoluminescence was observed in films of nanocrystalline silicon [3], as well as in thin films of  $\text{SiO}_2$  containing both crystalline [4,7,8,22] and amorphous [6] silicon nanoparticles.

Instrumental testing methods such as infrared spectroscopy and Raman scattering provide a rapid and non-destructive way to determine whether silicon particles are amorphous or crystalline [16,23]. In addition, information about the size of nanocrystallites can be obtained from the shape and position of the maximum of the first-order Raman scattering band [9,17]. In crystalline materials, this band usually takes the form of a Lorentzian line with an intrinsic linewidth of about  $3\text{ cm}^{-1}$  at room temperature. “Finite size effects” that break the overall translational symmetry of the material can lead to low-frequency asymmetric broadening and redshift of the Raman band. Thus, the size of nanoparticles can be determined from the details of the Raman line shape [9,11,18-20].

However, when using this approach, it is important to keep in mind that other factors such as structural damage, alloying, etc. can also cause similar changes [12,15]. In addition, the Raman line can be affected by tensile and compressive stresses, causing red and blue shifts, respectively.

### MATERIALS AND METHODS

In this study, n-Si-Dy composite was synthesized by thermal firing at  $1373\text{ K}$ . Infrared spectra and Raman studies were carried out on four samples, including n-Si and n-Si-Dy composites, which further confirmed the presence of both amorphous and nanocrystalline structures in films annealed at  $1373\text{ K}$ . Photoluminescence in the visible and near-infrared regions was observed in films containing both amorphous and crystalline particles.

To conduct the study, n-Si silicon samples with an initial resistance ranging from  $0.3$  to  $100\ \Omega\cdot\text{cm}$  were selected. The process of doping with dysprosium (Dy) impurities was carried out sequentially using the thermal diffusion method. The samples were chemically cleaned and etched with an HF solution to remove oxide layers from the surface.

Subsequently, films of high-purity Dy impurity (purity 99.999%) were deposited onto a clean silicon surface by vacuum deposition in evacuated quartz ampoules at a vacuum level of  $10^{-6}$  to  $10^{-8}$  Torr using an oil-free vacuum pumping system.

Diffusion annealing of the samples was performed at a temperature of 1373 K for 40 hours, followed by fast and slow cooling to uniformly dope the material and maximize the impurity concentration in silicon. Infrared (IR) spectra were obtained using a Bruker Invenio-X system in the wavenumber range from 400 to 4000  $\text{cm}^{-1}$  employing the attenuated total reflectance (ATR) method. Raman spectroscopy was conducted on a Bruker Senterra II Raman microscope using a 532 nm laser in the wavenumber range from 50 to 4265  $\text{cm}^{-1}$  at room temperature.

## RESULTS AND DISCUSSION

Thin films of dysprosium with high silicon content were successfully prepared by thermal calcination, and an n-Si-Dy composite was created by thermal baking at 1373 K. Raman measurements confirmed the formation of both amorphous and nanocrystalline structures in films annealed at 1373 K. Photoluminescence was observed and interpreted as interband recombination in nanoparticles larger than 2.5 nm, as well as carrier recombination through defect states in smaller nanoparticles.

FTIR spectra were carefully studied to identify structural changes in n-Si and the resulting n-Si-Dy compositions. The FTIR spectra of both the original n-Si and the resulting n-Si-Dy composite are presented in Figure 1.

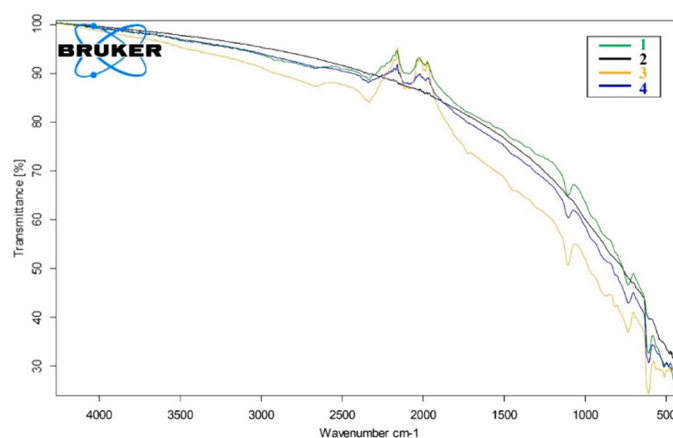


**Figure 1.** FTIR spectra of n-Si and the resulting n-Si<Dy>:

1. n-Si control: thermal firing at 1373 K for 40 hours, subsequent rapid cooling, without polishing;
2. n-Si<Dy> (fast cooling);
3. N-Si (starting material);
4. n-Si-Dy: thermal firing at 1373 K for 40 hours, followed by rapid cooling, with polishing

When analyzing n-Si itself, as well as n-Si-Dy composites obtained on its basis using FTIR spectrometry, in addition to the absorption of light on vibrations of regular atoms of the crystal lattice, in the solid there was also a process of absorption at local x fluctuations associated with defects and impurities. Thus, when analyzing the obtained FTIR spectra, the following patterns were revealed: absorption bands at 1106 and 515  $\text{cm}^{-1}$  of crystalline silicon are associated with the oxygen present in silicon (one must take into account the fact that oxygen in crystalline silicon is lies in the interstices and is an electrically neutral impurity insertion), carbon in crystalline silicon exhibits one antisymmetric stretching ( $\nu_{as}$ ) vibration, the frequency of which is 605  $\text{cm}^{-1}$ , peaks at 640  $\text{cm}^{-1}$  correspond to Si-H stretching, and peaks at 1615  $\text{cm}^{-1}$  - mode of perpendicular stretching. Dy-doped Si material exhibits additional peaks in its FTIR spectra due to the presence of vacancies and defects in n-Si<Dy> compositions. The peaks at 516.71  $\text{cm}^{-1}$  are due to the Si-Si stretching mode, while the peaks at 805  $\text{cm}^{-1}$  are due to the wagging mode of hydrogen. The frequency range (1950–2250  $\text{cm}^{-1}$ ) was deconvoluted to investigate potential local vibrational modes arising from defects and the formation of new bonds involving Dy.

Peaks located between 2210  $\text{cm}^{-1}$  and 2350  $\text{cm}^{-1}$  are typically attributed to Dy-Dy stretches. The peak at 2070  $\text{cm}^{-1}$  arises from adsorbed hydrogen at defective sites. Peaks at 2110  $\text{cm}^{-1}$  and 2124  $\text{cm}^{-1}$  correspond to Dy-Si and Si-Dy<sub>2</sub>, respectively [10]. Additionally, the peak at 2074  $\text{cm}^{-1}$  corresponds to db-Si-Si-H, where 'db' denotes dangling bonds. The small peak at 2211  $\text{cm}^{-1}$  may be attributed to Dy-induced microcrystallites.

To investigate changes in the FTIR spectra between the original n-Si and the resulting n-Si<Dy> compositions, we conducted a detailed study of the regions from 400 to 800  $\text{cm}^{-1}$  (refer to Figure 2). The resulting spectra clearly demonstrate all the changes occurring during the transition from n-Si to the resulting n-Si<Dy> compositions.

To further investigate the changes during the production of n-Si<Dy> compositions from the original n-Si, Raman spectroscopy was utilized. Raman spectra for four samples, including both n-Si and n-Si-Dy composites, obtained under different conditions and deposited on crystalline Si substrates annealed at 1373 K for 40 hours, are presented in Figure 3. A tail is observed, which does not develop into a distinct peak in any pattern. We assume that this tail is mainly due to scattering from silicon nanocrystals formed during annealing. This is confirmed by a similar low-energy tail observed in other Raman studies of silicon nanocrystals [12]. In these studies, the peak of the Raman band is slightly shifted relative to the Si single crystal band, but its low-energy tail is highly asymmetric and extends out to 450  $\text{cm}^{-1}$ , which is similar to

the tail of our Raman spectra (Figure 3). However, a small part of the scattering in the low-frequency tail of our spectra can be associated with n-Si, for which the Raman peak [10] at  $480\text{ cm}^{-1}$  asymmetrically extends to  $250 - 310\text{ cm}^{-1}$ . We do not observe any scattering below  $400\text{ cm}^{-1}$ , which means that most of the scattering in the low-energy tail of our spectra is due to Si nanocrystals. This conclusion is also confirmed by the results of X-ray diffraction (XRD), which show a fairly high density of Si nanocrystals in films annealed at  $1373\text{ K}$ .

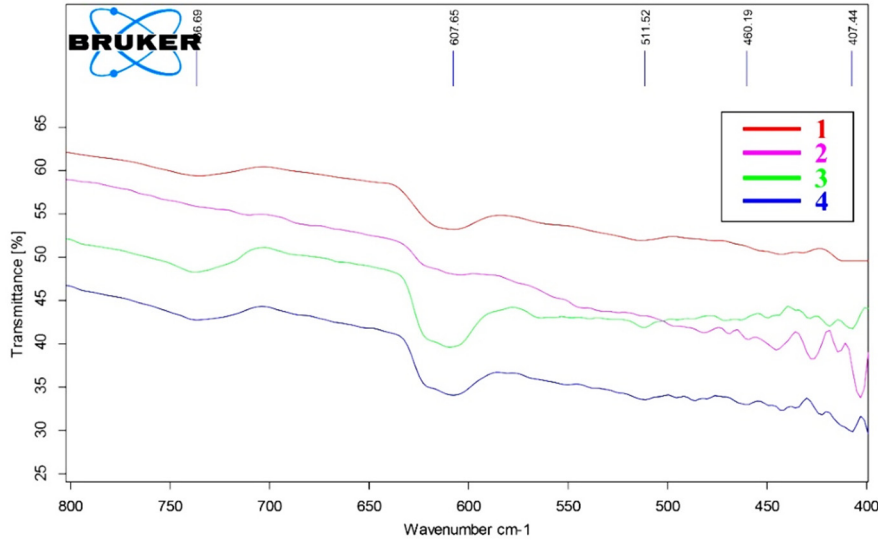


**Figure 2.** FTIR spectra of Si (spectrum region  $400\text{--}800\text{ cm}^{-1}$ ):

1. n-Si control: thermal firing at  $1373\text{ K}$  for 40 hours, subsequent rapid cooling, without polishing;
2. n-Si<Dy> (fast cooling);
3. N-Si (starting material);
4. n-Si-Dy: thermal firing at  $1373\text{ K}$  for 40 hours, followed by rapid cooling, with polishing

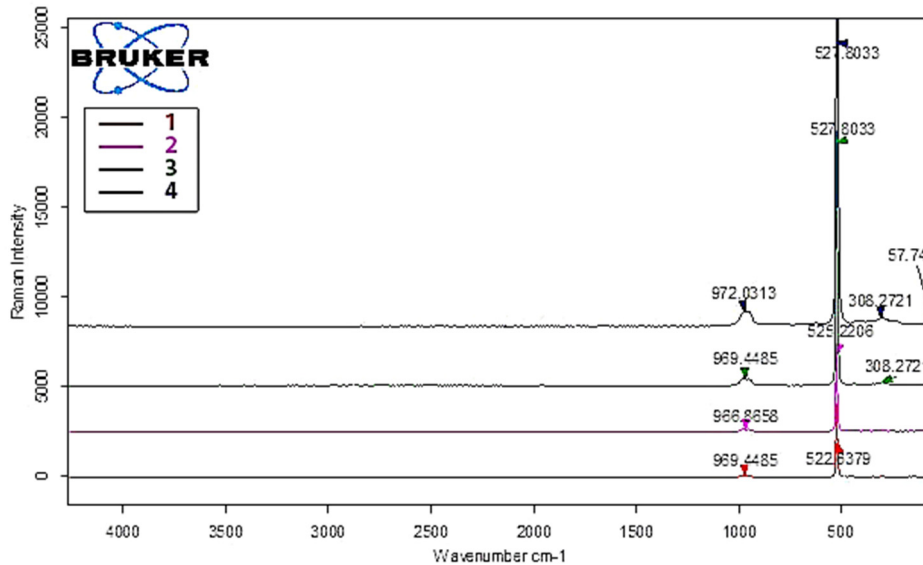


**Figure 3.** Raman spectra for four n-Si and n-Si<Dy> composite samples (range from  $50$  to  $4265\text{ cm}^{-1}$ ):

1. n-Si control: thermal firing at  $1373\text{ K}$  for 40 hours, subsequent rapid cooling, without polishing;
2. n-Si<Dy> (fast cooling);
3. N-Si (starting material);
4. n-Si-Dy: thermal firing at  $1373\text{ K}$  for 40 hours, followed by rapid cooling, with polishing

To analyze changes in the Raman spectrum between the original n-Si and the resulting n-Si<Dy> compositions, we conducted a detailed study of the regions from  $50$  to  $1400\text{ cm}^{-1}$  (refer to Figure 4). The resulting spectra clearly demonstrate all the changes occurring during the transition from n-Si to the resulting n-Si<Dy> compositions.

Based on the data presented in Figure 4, it is evident that the transition from the original n-Si to the resulting composites under different n-Si<Dy> conditions leads to changes in signals around  $307\text{ cm}^{-1}$  and  $960\text{ cm}^{-1}$ . These changes include increased intensity and mixing relative to the signals of the original n-Si. Additionally, the prominent signal in the region around  $522\text{ cm}^{-1}$  during this transition noticeably broadens, indicating a decrease in the crystallinity of the original n-Si.

Previous studies [14] have utilized Raman spectra to estimate the average size of Si and Dy nanocrystals. This can be achieved either by fitting the experimental curve with an expression accounting for finite size effects [14], or by using theoretically predicted dependencies [13] of band position and asymmetry on crystallite size.

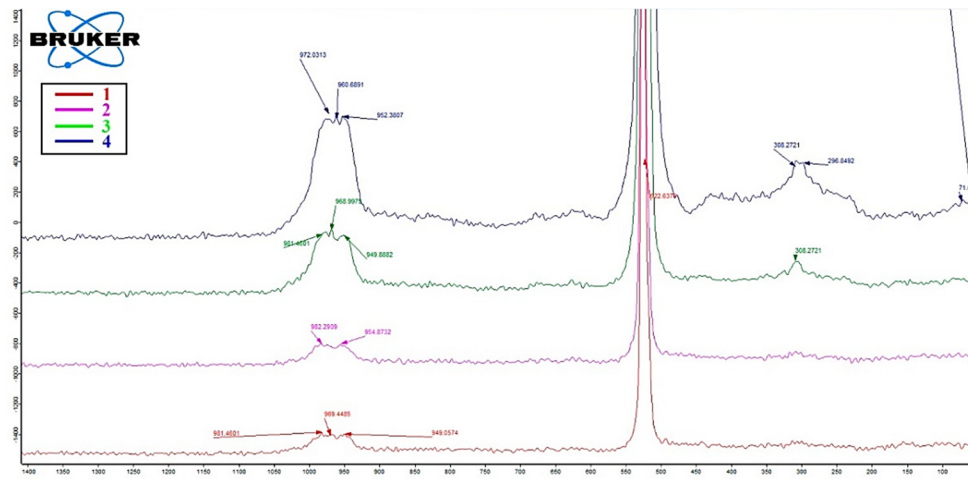


**Figure 4.** Raman spectra for four n-Si and n-Si<Dy> composite samples (range from 50 to 1400  $\text{cm}^{-1}$ ):

1. n-Si control: thermal firing at 1373 K for 40 hours, subsequent rapid cooling, without polishing;
2. n-Si<Dy> (fast cooling);
3. N-Si (starting material);
4. n-Si-Dy: thermal firing at 1373 K for 40 hours, followed by rapid cooling, with polishing

In both approaches, precise determination of the nanocrystal band is crucial, particularly for films grown on n-Si substrates where the  $522 \text{ cm}^{-1}$  band is also present in the Raman spectra. In nanocrystalline silicon films, the intensity of scattered light from the film is relatively high, while scattering from the substrate is significantly reduced due to absorption in the film. This ensures that the shape and position of the band originating from nanocrystals [10] are not distorted when scattered on the substrate. However, in Si-Dy films, the fill factor is relatively small, approximately 10% [7]. The intensity of scattered light from Si nanocrystals is low, whereas the Raman line due to the n-Si substrate remains strong. Figure 3 and 4 illustrate that a distinct band in all spectra peaks at  $522 \text{ cm}^{-1}$  with a width at half maximum of  $4.5 \text{ cm}^{-1}$ . It is evident that scattering from Si nanocrystals is weak and does not significantly impact the shape and position of the substrate signal. In an attempt to isolate the nanocrystal band, we subtracted the baseline, including background luminescence, noise, and the Lorentzian band with the aforementioned peak position and width at half maximum, from the measured spectrum of each film (Figure 3). Initially, the Lorentzian amplitude was set equal to the amplitude of the  $522 \text{ cm}^{-1}$  band in the measured spectra. However, due to the uncertainty in determining the exact intensity level of scattered light from the n-Si substrate, it is challenging to accurately determine the size of Si nanocrystals from the Raman spectra of Si-Dy thin films with a low fill factor.

## CONCLUSIONS

Characteristic peaks were identified in the FTIR spectra, such as the peak at  $640 \text{ cm}^{-1}$  associated with the Si-H mode and the peak at  $1615 \text{ cm}^{-1}$  associated with the perpendicular stretching mode, indicating specific structural features of the material. Additional peaks appeared in the FTIR spectra of n-Si-Dy samples, particularly at  $516.71 \text{ cm}^{-1}$  (Si-Si stretching mode) and  $805 \text{ cm}^{-1}$  (hydrogen wagging mode), suggesting the influence of dysprosium on the structure and properties of the material. These additional peaks indicate potential defects and vacancies in the new Si-Dy compositions, which are crucial for understanding changes in material structure.

Further analysis of the frequency ranges from  $1950$  to  $2250 \text{ cm}^{-1}$  confirmed the presence of local vibration modes associated with defects and the formation of new bonds involving dysprosium. Peaks related to Dy-Dy stretching were detected between  $2210 \text{ cm}^{-1}$  and  $2350 \text{ cm}^{-1}$ , indicating dysprosium interactions in the samples. The peak at  $2070 \text{ cm}^{-1}$  is attributed to adsorbed hydrogen at defect sites, which can influence material properties. Peaks at  $2110 \text{ cm}^{-1}$  (Dy-Si) and  $2124 \text{ cm}^{-1}$  (Si-Dy<sub>2</sub>) suggest the interaction of dysprosium with silicon in the samples. The peak at  $2074 \text{ cm}^{-1}$  corresponds to db-Si-Si-H, where db represents the dangling bond. Additionally, a peak at  $2211 \text{ cm}^{-1}$  may be attributed to dysprosium-induced microcrystals.

Regarding the Raman spectra, a “tail” is observed, which arises from scattering on silicon nanocrystals formed during annealing. This observation is consistent with the low-energy tail observed in other Raman studies of silicon nanocrystals. X-ray diffraction results confirm the high density of Si nanocrystals in films annealed at 1373 K. It's important to note that the observed scattering in the low-energy tail primarily originates from Si nanocrystals and not n-Si.

## ORCID

- © Khodjakbar S. Daliev, <https://orcid.org/0000-0002-2164-6797>; 
 © Sharifa B. Utamuradova, <https://orcid.org/0000-0002-1718-1122>  
 © Alisher Khaitbaev, <https://orcid.org/0000-0001-9892-8189>; 
 © Jonibek J. Khamdamov, <https://orcid.org/0000-0003-2728-3832>  
 © Shahriyor B. Norkulov, <https://orcid.org/0000-0002-2171-4884>; 
 © Mansur B. Bekmuratov, <https://orcid.org/0009-0006-3061-1568>

## REFERENCES

- [1] L.T. Canham, “Silicon quantum wire array fabrication by electrochemical and chemical dissolution of wafers,” *Appl. Phys. Lett.* **57**, 1046-1990. <https://doi.org/10.1063/1.103561>
- [2] F. Huisken, H. Hofmeister, B. Kohn, M.A. Laguna, and V. Paillard, “Laser production and deposition of light-emitting silicon nanoparticles,” *Appl. Surf. Sci.* **154–155**, 305 (2000). [https://doi.org/10.1016/s0169-4332\(99\)00476-6](https://doi.org/10.1016/s0169-4332(99)00476-6)

- [3] V. Vinciguerra, G. Franzo, F. Priolo, F. Iacona, and C. Spinella, "Quantum confinement and recombination dynamics in silicon nanocrystals embedded in Si/SiO<sub>2</sub> superlattices," *J. Appl. Phys.* **87**, 8165 (2000). <https://doi.org/10.1063/1.373513>
- [4] F. Koch, and V. Petrova-Koch, "Light from Si-nanoparticle systems - a comprehensive view," *J. Non-Cryst. Solids*, **198–200**, 840 (1996). [https://doi.org/10.1016/0022-3093\(96\)00067-1](https://doi.org/10.1016/0022-3093(96)00067-1)
- [5] Zh. Ma, X. Liao, J. He, W. Cheng, G. Yue, Y. Wang, and G. Kong, "Annealing behaviors of photoluminescence from SiO<sub>x</sub>:H," *J. Appl. Phys.* **83**, 7934 (1998). <https://doi.org/10.1063/1.367973>
- [6] M. Zaharias, H. Freistdt, F. Stolze, T.P. Drusedau, M. Rosenbauer, and M. Stutzmann, "Properties of sputtered a-SiO<sub>x</sub>:H alloys with a visible luminescence," *J. Non-Cryst. Solids*, **164–166**, 1089 (1993). [https://doi.org/10.1016/0022-3093\(93\)91188-9](https://doi.org/10.1016/0022-3093(93)91188-9)
- [7] U. Kahler, and H. Hofmeister, "Silicon nanocrystallites in buried SiO<sub>x</sub> layers via direct wafer bonding," *Appl. Phys. Lett.* **75**, 641 (1999). <https://doi.org/10.1063/1.124467>
- [8] S. Zhang, W. Zhang, and J. Yuan, "The preparation of photoluminescent Si nanocrystal–SiO<sub>x</sub> films by reactive evaporation," *Thin Solid Films*, **326**, 92 (1998). [https://doi.org/10.1016/S0040-6090\(98\)00532-X](https://doi.org/10.1016/S0040-6090(98)00532-X)
- [9] H. Richter, Z.P. Wang, and L. Ley, "The one phonon Raman spectrum in microcrystalline silicon," *Solid State Commun.* **39**, 625 (1981). [https://doi.org/10.1016/0038-1098\(81\)90337-9](https://doi.org/10.1016/0038-1098(81)90337-9)
- [10] Z. Iqbal, and S. Veprek, "Raman scattering from hydrogenated microcrystalline and amorphous silicon," *J. Phys. C*, **15**, 377 (1982). <https://doi.org/10.1088/0022-3719/15/2/019>
- [11] J. Gonzales-Hernandez, G.H. Azarbayejani, R. Tsu, and F.H. Pollak, "Raman, transmission electron microscopy, and conductivity measurements in molecular beam deposited microcrystalline Si and Ge: A comparative study," *Appl. Phys. Lett.* **47**, 1350 (1985). <https://doi.org/10.1063/1.96277>
- [12] I.H. Campbell, and P.M. Fauchet, "The effects of microcrystal size and shape on the one phonon Raman spectra of crystalline semiconductors," *Solid State Commun.* **52**, 739 (1986). [https://doi.org/10.1016/0038-1098\(86\)90513-2](https://doi.org/10.1016/0038-1098(86)90513-2)
- [13] J. Zi, H. Buscher, C. Falter, W. Ludwig, K. Zhang, and X. Xie, "Raman shifts in Si nanocrystals," *Appl. Phys. Lett.* **69**, 200 (1996). <https://doi.org/10.1063/1.117371>
- [14] D.R. dos Santos, and I.L. Torriani, "Crystallite size determination in μc-Ge films by x-ray diffraction and Raman line profile analysis," *Solid State Commun.* **85**, 307 (1993). [https://doi.org/10.1016/0038-1098\(93\)90021-E](https://doi.org/10.1016/0038-1098(93)90021-E)
- [15] Kh.S. Daliev, Z.E. Bahronkulov, and J.J. Hamdamov, "Investigation of the Magnetic Properties of Silicon Doped with Rare-Earth Elements," *East Eur. J. Phys.* **4**, 167 (2023). <https://doi.org/10.26565/2312-4334-2023-4-18>
- [16] Kh.S. Daliev, Sh.B. Utamuradova, Z.E. Bahronkulov, A.Kh. Khaitbaev, and J.J. Hamdamov, "Structure Determination and Defect Analysis n-Si<Lu>, p-Si<Lu> Raman Spectrometer Methods," *East Eur. J. Phys.* **4**, 193 (2023). <https://doi.org/10.26565/2312-4334-2023-4-23>
- [17] P.A. Temple, and C.E. Hathaway, "Multiphonon Raman Spectrum of Silicon," *Physical Review B*, **7(8)**, 3685–3697 (1973). <https://doi.org/10.1103/PhysRevB.7.3685>
- [18] K.J. Kingma, and R.J. Hemley, "Raman spectroscopic study of microcrystalline silica," *American Mineralogist*, **79(3-4)**, 269–273 (1994). [https://pubs.geoscienceworld.org/msa/ammin/article-pdf/79/3-4/269/4209223/am79\\_269.pdf](https://pubs.geoscienceworld.org/msa/ammin/article-pdf/79/3-4/269/4209223/am79_269.pdf)
- [19] G.E. Walrafen, Y.C. Chu, and M.S. Hokmabadi, "Raman spectroscopic investigation of irreversibly compacted vitreous silica," *The Journal of Chemical Physics*, **92(12)**, 6987–7002 (1990). <https://doi.org/10.1063/1.458239>
- [20] B. Champagnon, C. Martinet, M. Boudeulle, D. Vouagner, C. Coussa, T. Deschamps, and L. Grosvalet, "High pressure elastic and plastic deformations of silica: in situ diamond anvil cell Raman experiments," *Journal of Non-Crystalline Solids*, **354(2-9)**, 569–573 (2008). <https://doi.org/10.1016/j.jnoncrysol.2007.07.079>
- [21] A.S. Zakirov, Sh.U. Yuldashev, H.J. Wang, H.D. Cho, T.W. Kang, J.J. Khamdamov, and A.T. Mamadalimov, "Photoluminescence study of the surface modified and MEH-PPV coated cotton fibers," *Journal of Luminescence*, **131(2)**, 301–305 (2011). <https://doi.org/10.1016/j.jlumin.2010.10.019>
- [22] Sh.B. Utamuradova, H.J. Matchonov, Zh.J. Khamdamov, and H.Yu. Utemuratova, "X-ray diffraction study of the phase state of silicon single crystals doped with manganese," *New Materials, Connections Oath Applications*, **7(2)**, 93–99 (2023). [http://jomardpublishing.com/UploadFiles/Files/journals/NMCA/v7n2/Utamuradova\\_et\\_al.pdf](http://jomardpublishing.com/UploadFiles/Files/journals/NMCA/v7n2/Utamuradova_et_al.pdf)
- [23] Kh.S. Daliev, Sh.B. Utamuradova, J.J. Khamdamov, M.B. Bekmuratov, "Structural Properties of Silicon Doped Rare Earth Elements Ytterbium," *East Eur. J. Phys.* **1**, 375–379 (2024). <https://doi.org/10.26565/2312-4334-2024-1-37>

### ДЕФЕКТНА СТРУКТУРА КРЕМНІЮ, ЛЕГОВАНОГО ДИСПРОЗІЄМ

Ходжакбар С. Далієв<sup>а</sup>, Шаріфа Б. Утамурадова<sup>б</sup>, Алішер Хайтбаєв<sup>б</sup>, Джонібек Дж. Хамдамов<sup>б</sup>,  
Шахрійор Б. Норкулов<sup>б</sup>, Мансур Б. Бекмуратов<sup>с</sup>

<sup>а</sup>Філія Федерального державного бюджетного навчального закладу вищої освіти «Національний дослідницький університет МПЕІ», вул. Йогду, 1, м. Ташкент, Узбекистан

<sup>б</sup>Інститут фізики напівпровідників та мікроелектроніки Національного університету Узбекистану, 100057, Ташкент, Узбекистан, вул. Янги Алмазар, 20

<sup>с</sup>Нукусський державний педагогічний інститут імені Аджиніяза, Нукус, Узбекистан

У цій роботі було проаналізовано структурні та оптичні характеристики зразків кремнію (n-Si) та його композиції з диспрозієм (n-Si-Dy) за допомогою методів інфрачервоної спектроскопії з перетворенням Фур'є (FTIR) та спектроскопії раманівського розсіювання. Були ідентифіковані характерні піки в спектрах FTIR, такі як 640 см<sup>-1</sup> (режим Si-H) і 1615 см<sup>-1</sup> (режим перпендикулярного розтягування), що вказує на структурні особливості матеріалу. Поява додаткових піків у спектрах n-Si-Dy при 516,71 см<sup>-1</sup> та 805 см<sup>-1</sup> свідчить про вплив диспрозію на структуру та дефектність матеріалу. Дослідження частотного діапазону (1950–2250 см<sup>-1</sup>) додатково підтверджує локальні моди вібрації, пов'язані з дефектами та взаємодією з диспрозієм. Піки, пов'язані з розтягуванням Ду-Ду, а також взаємодією з кремнієм, були знайдені при 2110 см<sup>-1</sup> і 2124 см<sup>-1</sup>. Аналіз спектрів комбінаційного розсіювання свідчить про утворення нанокристалів кремнію під час відпалу, що підтверджено результатами XRD. Отримані результати дають важливе уявлення про вплив диспрозію на структуру та властивості кремнієвих матеріалів, які потенційно можуть знайти застосування в оптоелектроніці та матеріалознавстві.

**Ключові слова:** кремній; диспрозій; рідкоземельні елементи; комбінаційне розсіювання; дифузія; термообробка; температура